

Photoluminescence study of Sb-doped *p*-type ZnO films by molecular-beam epitaxy

F. X. Xiu, Z. Yang, L. J. Mandalapu, D. T. Zhao, and J. L. Liu^{a)}

Quantum Structures Laboratory, Department of Electrical Engineering, University of California, Riverside, California 92521

(Received 7 September 2005; accepted 10 November 2005; published online 12 December 2005)

We investigated photoluminescence (PL) from reliable and reproducible Sb-doped *p*-type ZnO films grown on *n*-Si (100) by molecular-beam epitaxy. Well-resolved PL spectra were obtained from completely dopant-activated samples with hole concentrations above $1.0 \times 10^{18} \text{ cm}^{-3}$. From free electron to acceptor transitions, acceptor binding energy of 0.14 eV is determined, which is in good agreement with analytical results of the temperature-dependent PL measurements. Another broad peak at 3.050 eV, which shifts to lower energy at higher temperatures, indicates the formation of deep acceptor level bands related to Zn vacancies, which are created by Sb doping. © 2005 American Institute of Physics. [DOI: 10.1063/1.2146208]

ZnO has been recognized as a promising material for optoelectronic devices, such as ultraviolet light-emitting diodes, laser diodes, and photodetectors, owing to its wide band gap of 3.37 eV and large exciton binding energy of 60 meV at room temperature.^{1,2} Although many groups have successfully achieved *p*-type ZnO by doping with N,³⁻⁹ P,¹⁰⁻¹³ and As,¹⁴⁻¹⁷ the reliability and reproducibility are still the main issues that hinder the development of ZnO-based optoelectronic devices. Recently, we started to grow ZnO by Sb doping with an electron cyclotron resonance (ECR)-assisted molecular-beam epitaxy (MBE), and reliable and reproducible *p*-type doping was proved using Hall effect electrical characterizations.¹⁸ In this letter, we focus on the optical properties of Sb-doped ZnO films with different Sb effusion cell temperatures and different annealing conditions to reveal its doping mechanism.

Undoped and Sb-doped ZnO films were grown on *n*-Si (100) substrates at 550 °C under oxygen-rich conditions. All active layers were 200 nm thick. The detailed growth procedures were reported elsewhere.¹⁸ For the undoped ZnO film, after growth, an annealing process was performed at 800 °C for 30 min under vacuum. For Sb-doped ZnO films, two series of samples were prepared with different growth conditions, as shown in Table I. The first series of samples (B–D) were grown with different Sb effusion cell temperatures of 300, 330, and 350 °C, respectively, and were *in situ* annealed at the temperature of 800 °C for 30 min. Room temperature Hall measurements show that the undoped ZnO (sample A) has an *n*-type conductivity with a carrier concentration of $5.0 \times 10^{18} \text{ cm}^{-3}$ and a mobility of 95.6 $\text{cm}^2/\text{V s}$. The Sb-doped ZnO films, however, show strong *p*-type conductivities. With an Sb effusion cell temperature of 300 °C (sample B), the film exhibits a carrier concentration of $1.3 \times 10^{17} \text{ cm}^{-3}$ and a mobility of 28.0 $\text{cm}^2/\text{V s}$. By increasing the Sb effusion cell temperature to 330 °C (sample C), the carrier concentration increases to $6.0 \times 10^{17} \text{ cm}^{-3}$ while the mobility decreases to 25.9 $\text{cm}^2/\text{V s}$. Further raising the Sb effusion cell temperature to 350 °C results in an even higher

carrier concentration of $1.7 \times 10^{18} \text{ cm}^{-3}$ and a lower mobility of 20.0 $\text{cm}^2/\text{V s}$ (sample D).

The second series of samples (D–G) were grown with the same Sb effusion cell temperature of 350 °C, but they were annealed for 30 min at different temperatures of 800, 600, 700, and 840 °C, respectively. It is evident that the annealing temperature plays a very important role in the electrical properties of Sb-doped films, as shown in Table I. With an annealing temperature of 600 °C (sample E), the film shows *p*-type conductivity with a low carrier concentration of $4.9 \times 10^{17} \text{ cm}^{-3}$ and a high mobility of 27.3 $\text{cm}^2/\text{V s}$. By raising the annealing temperatures above 700 °C (samples F, D, and G), the carrier concentrations tend to be saturated ($\sim 1.0 \times 10^{18} \text{ cm}^{-3}$), indicating that all Sb dopants are activated. The lowest resistivity of 0.2 $\Omega \text{ cm}$ was obtained with Sb effusion cell temperature of 350 °C and annealing temperature above 700 °C for 30 min (samples F, D, and G).

PL measurements were carried out to characterize optical properties of undoped and Sb-doped ZnO films using a 325 nm He–Cd laser with an excitation power of 5 mW. Figure 1 shows a PL spectrum for the undoped ZnO film (sample A) at 8.5 K. A strong near-band edge emission associated with the neutral-donor-bound exciton (D^0X) is observed at 3.353 eV. A free-exciton related emission at 3.380 eV is also seen and identified as the ground state of A exciton,¹⁹ denoted as $FX_A^{n=1}$. Another emission occurs at

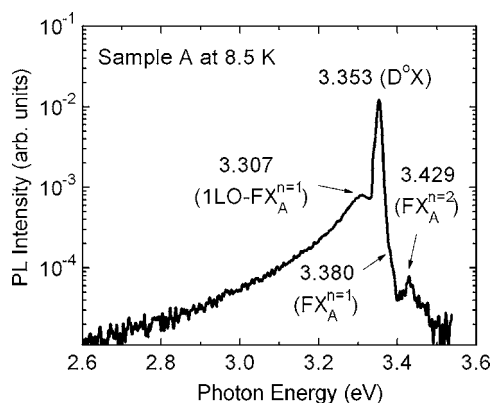


FIG. 1. A PL spectrum at $T=8.5 \text{ K}$ for the undoped ZnO film (sample A).

^{a)} Author to whom correspondence should be addressed; electronic mail: jianlin@ee.ucr.edu

TABLE I. Electrical properties at room temperature of undoped and Sb-doped ZnO films.

Sample	Sb cell temperature (°C)	Type	Mobility (cm ² /V s)	Resistivity (Ω cm)	Carrier density (cm ⁻³)	Annealing temperature (°C)
A	Undoped	<i>n</i>	95.6	0.01	5.0×10^{18}	800
B	300	<i>p</i>	28.0	1.7	1.3×10^{17}	800
C	330	<i>p</i>	25.9	0.3	6.0×10^{17}	800
D	350	<i>p</i>	20.0	0.2	1.7×10^{18}	800
E	350	<i>p</i>	27.3	0.5	4.9×10^{17}	600
F	350	<i>p</i>	22.6	0.2	1.1×10^{18}	700
G	350	<i>p</i>	20.0	0.2	1.8×10^{18}	840

3.429 eV, which may be attributed to the first state of A exciton,¹⁹ denoted as $FX_A^{n=2}$. It is reported that the LO phonon replica occurs with a separation of 71–73 meV.¹⁹ As a result, the emission at 3.307 eV is ascribed to the LO-phonon replica of the ground state A exciton, denoted as $1LO - FX_A^{n=1}$. The observation of different states of free exciton in the undoped ZnO film indicates that the ZnO film grown on the Si (100) substrate is of high quality.

Figure 2 shows PL spectra at $T=8.5$ K for Sb-doped ZnO films (samples B–G). In Fig. 2(a), doping effects on PL emissions are shown. With a Sb effusion cell temperature of 300 °C (sample B), the film shows the dominated emissions at 3.358 and 3.220 eV, corresponding to natural-acceptor-bound exciton (A^0X) and donor-acceptor pair (DAP) transition, respectively.¹⁸ With a higher Sb effusion cell temperature of 330 °C (sample C), the DAP emission becomes stronger. By further raising the Sb effusion cell temperature to 350 °C (sample D), the PL spectrum shows well-resolved emissions at 3.358 (A^0X), 3.296 (FA) and 3.222 eV (DAP). Besides these peaks, it is interesting to note that a strong and broad emission is found at 3.050 eV for sample D.

To further understand this emission, the dopant activation was performed at different annealing temperatures for heavily Sb-doped ZnO films as shown in Fig. 2(b). With an annealing temperature of 600 °C (sample E), the film shows a broad emission at 3.358 eV (A^0X) compared to the undoped ZnO film (sample A), which is attributed to homogeneous broadening as a result of the extensive incorporation of large-size Sb atoms into the ZnO crystals. With an annealing temperature of 700 °C (sample F), the emission line of 3.050 eV starts to show up. Raising the annealing temperature above 800 °C results in the appearance of FA transition

and clear emission-line at 3.050 eV (samples D and G). The difference between samples D and G is negligible, indicating the complete activation of Sb dopants for the annealing temperature above 800 °C. The emission at 3.050 eV is related to Zn vacancies (V_{Zn}).²⁰ With the complete activation of Sb dopants at the annealing temperature of 800 °C or above, heavy Sb doping facilitates the formation of more Zn vacancies than light Sb doping, leading to more significant Zn vacancy-related peak. Owing to the large size of the Sb atom, instead of replacing an oxygen atom, a Sb dopant was predicted to substitute a Zn atom and simultaneously connect two Zn vacancies to form a $Sb_{Zn}-2V_{Zn}$ complex, which is a shallow acceptor.²¹ In our experiments, it is observed that Sb doping can result in the formation of Zn vacancies; thus the complex $Sb_{Zn}-2V_{Zn}$ could be the explanation of strong *p*-type conductivity. In addition, the observation of evident Zn vacancy-related emission at 3.050 eV indicates that, with heavy Sb doping, there are more Zn vacancies induced than needed to participate in the complex. However, these Zn vacancies do not play important roles in *p*-type conductivity since they are relatively deeper acceptors than the complex $Sb_{Zn}-2V_{Zn}$.

To obtain the acceptor binding energy of Sb-doped ZnO films, the temperature-dependent PL measurements were performed on sample G from 8.5 to 300 K, as shown in Fig. 3. With an increase of the temperature from 8.5 to 100 K, emissions at 3.296 and 3.222 eV (at 8.5 K) show blue shifts, which are typical characteristics of FA and DAP transitions.²² Moreover, over the whole temperature range, 3.222 eV emission-line progressively merges into 3.296 eV emission-line, showing the feature of the thermal ionization

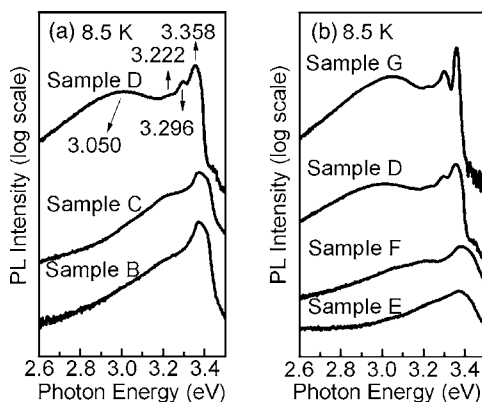


FIG. 2. PL spectra at $T=8.5$ K for Sb-doped ZnO films (samples B–G) with different growth conditions, as shown in Table I.

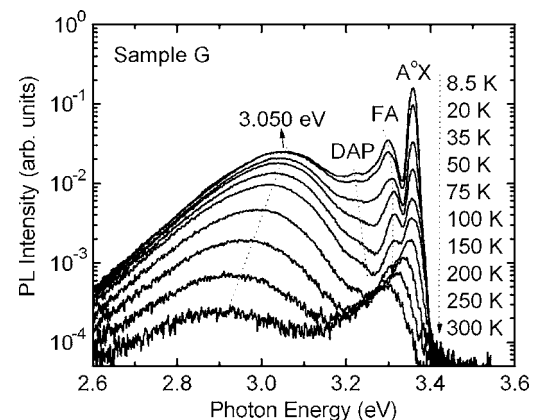


FIG. 3. PL spectra measured at several temperatures over the range from 8.5 to 300 K for sample G.

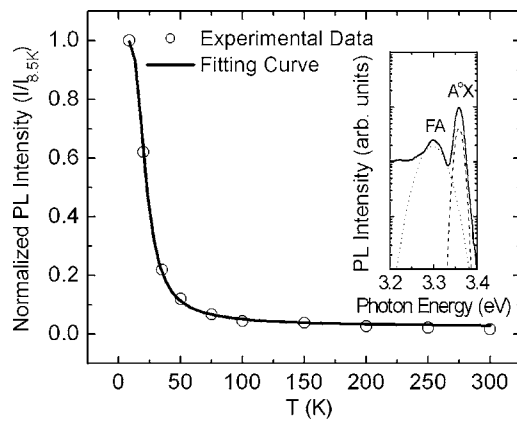


FIG. 4. The integrated intensity of the A^0X emission as a function of temperature for sample G. The circles represent the experimental data, and the solid line is the fitting to Eq. (2). The inset shows that the spectrum (sample G at $T=20$ K, solid line) is resolved into two individual peaks by using a multi-Gaussian fitting, which correspond to the A^0X emission (dashed line) and the FA emission (dotted line).

of donors.²³ Therefore, these two emissions at 3.296 and 3.222 eV are identified as FA and DAP transitions, respectively. The emission around 3.050 eV shows a redshift with the increase of temperature, indicating that the deep acceptor levels associated with Zn vacancies as a result of Sb doping may have formed a band. The appearance of the FA emission enables us to calculate the acceptor binding energy (E_A) at 8.5 K with^{14,22}

$$E_A = E_{\text{gap}} - E_{\text{FA}} + k_B T/2, \quad (1)$$

where E_{FA} is the temperature-dependent transitions, and $E_{\text{FA}}=3.296$ eV at 8.5 K. With an intrinsic band gap of $E_{\text{gap}}=3.437$ eV at 8.5 K,^{23,24} the value of E_A is calculated to be 0.14 eV. This is slightly smaller than 0.2 eV based on the DAP transition in our previous study.¹⁸ However, this is possible as the energy position of the DAP band can only give a rough estimate of the acceptor binding energy because of the inaccurate determination of the donor to acceptor distance.²²

Figure 4 shows the integrated intensity of the A^0X emission as a function of temperature for sample G. The temperature dependence of the integrated PL intensity is given by²⁵

$$I(T) = I_0 [1 + C \exp(-E_b^{A^0X}/kT)], \quad (2)$$

where C is a fitting parameter, I_0 is the integrated PL intensity at zero temperature, which is approximately the same as at $T=8.5$ K, and $E_b^{A^0X}$ is the binding energy between the acceptor and free exciton. From the fitting to Eq. (2), $E_b^{A^0X}=15$ meV was obtained. Using the Haynes rule $E_b^{A^0X}/E_A \approx 0.1$ for ZnO material system,^{15,18} an acceptor binding energy E_A is estimated to be 0.15 eV. This result is in good agreement with the value for the acceptor level obtained from spectroscopic data using Eq. (1).

In summary, reliable and reproducible Sb-doped p -type ZnO thin films were grown on n -Si (100) by ECR-assisted MBE. PL was used to systematically investigate the films grown with different Sb effusion cell temperatures and different annealing conditions. The results show that well-resolved PL spectra can be obtained with the hole concentration above $1.0 \times 10^{18} \text{ cm}^{-3}$ and the annealing temperature

above 800 °C, which is corresponding to the complete activation of Sb dopants. The appearance of FA transition at 3.296 eV allows the determination of acceptor binding energy of 0.14 eV, which is in good agreement with the results of the temperature-dependent PL measurements. In addition, heavy Sb doping creates more Zn vacancies than $\text{Sb}_{\text{Zn}}-2\text{V}_{\text{Zn}}$ complexes require, as indicated from 3.050 eV emissions. These experimental results further demonstrate that Sb is an excellent candidate for the reliable p -type ZnO fabrication.

This work was supported by DARPA/DMEA through the center for NanoScience and Innovation for Defense (CNID) under the Award No. H94003-04-2-0404. The authors would also like to acknowledge Joo-Young Lee (at UCLA, EE Department) for his assistance on room temperature Hall measurements.

¹D. C. Look, Mater. Sci. Eng., B **80**, 383 (2001).

²S. J. Pearton, D. P. Norton, K. Ip, Y. W. Heo, and T. Steiner, J. Vac. Sci. Technol. B **22**, 932 (2004).

³A. Tsukazaki, A. Ohtomo, T. Onuma, M. Ohtani, T. Makino, M. Sumiya, K. Ohtani, S. F. Chichibu, S. Fuke, Y. Segawa, H. Ohno, H. Koinuma, and M. Kawasaki, Nat. Mater. **4**, 42 (2005).

⁴J. M. Bian, X. M. Li, C. Y. Zhang, W. D. Yu, and X. D. Gao, Appl. Phys. Lett. **85**, 4070 (2004).

⁵D. C. Look, D. C. Reynolds, C. W. Litton, R. L. Jones, D. B. Eason, and G. Cantwell, Appl. Phys. Lett. **81**, 1830 (2002).

⁶H. W. Liang, Y. M. Lu, D. Z. Shen, Y. C. Liu, J. F. Yan, C. X. Shan, B. H. Liu, Z. Z. Zhang, J. Y. Zhang, and X. W. Fan, Phys. Status Solidi A **202**, 1060 (2005).

⁷J. G. Lu, Z. Z. Ye, F. Zhuge, Y. J. Zeng, B. H. Zhao, and L. P. Zhu, Appl. Phys. Lett. **85**, 3134 (2004).

⁸E. Kamińska, A. Piotrowska, J. Kossut, R. Butkutė, W. Dobrowolski, R. Łukasiewicz, A. Barcz, R. Jakiela, E. Dynowska, E. Przeździecka, M. Aleszkiewicz, P. Wojnar, and E. Kowalczyk, Phys. Status Solidi C **2**, 1119 (2005).

⁹X. Li, Y. Yan, T. A. Gessert, C. L. Perkins, D. Young, C. DeHart, M. Young, and T. J. Coutts, J. Vac. Sci. Technol. A **21**, 1342 (2003).

¹⁰D. K. Hwang, H. S. Kim, J. H. Lim, J. Y. Oh, J. H. Yang, S. J. Park, K. K. Kim, D. C. Look, and Y. S. Park, Appl. Phys. Lett. **86**, 151917 (2005).

¹¹V. Vaithianathan, B. T. Lee, and S. S. Kim, Phys. Status Solidi A **201**, 2837 (2004).

¹²K. K. Kim, H. S. Kim, D. K. Hwang, J. H. Lim, and S. J. Park, Appl. Phys. Lett. **83**, 63 (2003).

¹³Z. Q. Chen, A. Kawasuso, Y. Xu, H. Naramoto, X. L. Yuan, T. Sekiguchi, R. Suzuki, and T. Ohdaira, J. Appl. Phys. **97**, 013528 (2005).

¹⁴Y. R. Ryu, T. S. Lee, and H. W. White, Appl. Phys. Lett. **83**, 87 (2003).

¹⁵D. C. Look, G. M. Renlund, R. H. Burgener II, and J. R. Sizelove, Appl. Phys. Lett. **85**, 5269 (2004).

¹⁶V. Vaithianathan, B. T. Lee, and S. S. Kim, Appl. Phys. Lett. **86**, 062101 (2005).

¹⁷T. S. Jeong, M. S. Han, C. J. Youn, and Y. S. Park, J. Appl. Phys. **96**, 175 (2004).

¹⁸F. X. Xiu, Z. Yang, L. J. Mandalapu, D. T. Zhao, J. L. Liu, and W. P. Beyermann, Appl. Phys. Lett. **87**, 152101 (2005).

¹⁹A. Teke, Ü. Özgür, S. Doğan, X. Gu, and H. Morkoç, Phys. Rev. B **70**, 195207 (2004).

²⁰B. X. Lin, Z. X. Fu, and Y. B. Jia, Appl. Phys. Lett. **79**, 943 (2001).

²¹S. Limpijumnong, S. B. Zhang, S. H. Wei, and C. H. Park, Phys. Rev. Lett. **92**, 155504 (2004).

²²K. Tamura, T. Makino, A. Tsukazaki, M. Sumiya, S. Fuke, T. Furumochi, M. Lippmaa, C. H. Chia, Y. Segawa, H. Koinuma, and M. Kawasaki, Solid State Commun. **127**, 265 (2003).

²³B. K. Meyer, H. Alves, D. M. Hofmann, W. Kriegseis, D. Forster, F. Bertram, J. Christen, A. Hoffmann, M. Straßburg, M. Dworzak, U. Haboeck, and A. V. Rodina, Phys. Status Solidi B **241**, 231 (2004).

²⁴L. J. Wang and N. C. Giles, J. Appl. Phys. **94**, 973 (2003).

²⁵M. Leroux, N. Grandjean, B. Beaumont, G. Nataf, F. Semond, J. Massies, and P. Gibart, J. Appl. Phys. **86**, 3721 (1999).